

Technical Note: Electrochemistry of CO₂ Corrosion of Mild Steel: Effect of CO₂ on Cathodic Currents

Aria Kahyarian,^{‡*} Bruce Brown,^{*} and Srdjan Nešić^{*}

ABSTRACT

The common understanding of aqueous CO₂ corrosion mechanism considers carbonic acid as an electroactive species. The direct reduction of carbonic acid on a steel surface is believed to be the cause of the higher corrosion rates of mild steel, as compared to that observed in strong-acid solutions with the same pH. However, in-depth quantitative analyses based on comprehensive mechanistic models, developed in recent years, have challenged this idea. In an attempt to provide explicit experimental evidence for the significance of direct reduction of carbonic acid in CO₂ corrosion of mild steel, the charge transfer controlled cathodic currents in CO₂ saturated solutions were investigated in the present study. The experiments were conducted on three different surfaces: Type 316L stainless steel, pure iron, and API 5L X65 mild steel, in order to examine the possible effect of alloying impurities on the kinetics and the mechanism of cathodic currents. The experimental polarization curves showed that at a constant pH, the charge transfer controlled cathodic currents did not increase with increasing partial pressure of CO₂ from 0 bar to 5 bar. This confirmed that the direct carbonic acid reduction was not significant at the conditions covered in the present study, and its sole effect was to buffer the hydrogen ion concentration.

KEY WORDS: carbon dioxide, carbon steel, cathodic polarization, stainless steel

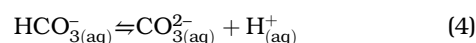
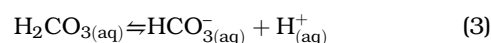
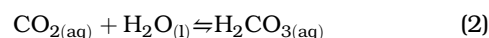
Submitted for publication: February 20, 2018. Revised and accepted: March 23, 2018. Preprint available online: March 23, 2018. <https://doi.org/10.5006/2792>.

[‡] Corresponding author. E-mail: ak702711@ohio.edu.

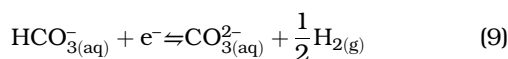
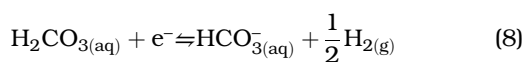
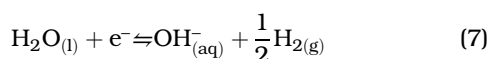
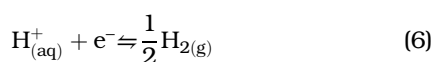
^{*} Institute for Corrosion and Multi-Phase Flow Technology, Ohio University, 342 West State Street, Athens, OH 45701.

INTRODUCTION

The mechanism of cathodic reactions involved in CO₂ corrosion, i.e., the sequence of electrochemical and chemical reactions, is a rather complex matter, in the sense that it involves a number of electroactive species that are interrelated through homogeneous chemical reactions. The CO₂ gas, upon dissolution in water (Reaction [1]), goes through hydration (Reaction [2]) and dissociation reactions (Reactions [3] and [4]) to form an acidic, corrosive solution.



The CO₂ corrosion in aqueous acid solutions is generally believed to involve numerous electrochemical reactions as shown below.¹⁻³ Anodic partial of Reaction (5) is the cause of metal deterioration, and cathodic partial of Reactions (6) through (9) provide the electron sink required for the anodic reaction to progress spontaneously. The significance of these reactions is mainly based on the studies done by de Waard and Milliams in 1975,⁴⁻⁵ Schmitt and Rothmann in 1977,⁶ and Gray, et al., in 1989 and 1990,⁷⁻⁸ as reviewed in more details elsewhere.⁹⁻¹¹



The profound effect of homogeneous reactions is mainly associated with the CO_2 hydration equilibrium, where only a small fraction ($\sim 0.2\%$) of $\text{CO}_{2(\text{aq})}$ reacts to form H_2CO_3 .¹ Therefore, there is a large reservoir of $\text{CO}_{2(\text{aq})}$ present in the solution to replenish the H_2CO_3 concentration as it is consumed by the corrosion process. The higher corrosion rates observed in aqueous CO_2 solutions, as compared to a strong acid solution (e.g., HCl) at the same pH, were therefore associated with the additional H_2CO_3 reduction and the effect of CO_2 hydration reaction.¹⁰⁻¹²

While the abovementioned mechanistic view of the cathodic reactions in CO_2 corrosion is widely accepted, the findings in more recent studies have challenged its basis.¹³⁻¹⁵ In those studies it was shown quantitatively that the limiting currents could be adequately explained even if H_2CO_3 was not considered an electroactive species.¹³⁻¹⁵ This can be understood when considering the local concentration of chemical species at the metal surface, and the influence of the homogeneous chemical reactions. That is, the H_2CO_3 dissociation reaction (Reaction [3]) occurs in the vicinity of the metal surface, followed by electrochemical reduction of the produced H^+ ions (Reaction [6]), which provides a parallel reaction pathway to the direct H_2CO_3 reduction reaction. This observation carries a significant mechanistic implication, because it undermines the previous commonly accepted mechanistic arguments, which were developed based on the analysis of cathodic polarization behavior at or close to limiting currents.⁶⁻⁸ Therefore, to date, the evidence for direct H_2CO_3 reduction is mostly circumstantial. This was perhaps best noted by Nordsveen, et al.,¹³ who suggested that while the cathodic limiting currents can be quantitatively explained without considering H_2CO_3 as an electroactive species, the predicted corrosion rates are in better agreement with the experimental data when this additional reaction was included in the model.

The electrochemical activity of H_2CO_3 has been discussed specifically in a few different studies. Linter and Burstein published one of the earliest articles suggesting that H_2CO_3 is not electrochemically active.¹⁶ The authors investigated the mechanism of CO_2 corrosion on both a 13Cr stainless steel and a low alloy

steel. The arguments were developed based on the polarization curves obtained in N_2 -saturated and CO_2 -saturated 0.5 M NaCl solutions at pH 4.0 with additional potassium hydrogen phthalate buffer. In a nutshell, the authors were able to observe the charge transfer controlled current densities at both N_2 -saturated and CO_2 -saturated solutions. The results showed no significant increase in this range of current densities when comparing the two solutions, leading to the conclusion that H_2CO_3 is not electrochemically active. The findings of Linter and Burstein¹⁶ did not gain much attention over the years, perhaps because of the concerns arising from the limited environmental conditions covered in their study—i.e., the fact that at pH 4.0 the cathodic current is dominated by H^+ reduction. The concentration of H_2CO_3 at 1 bar (100 kPa) CO_2 is about a third of H^+ at pH 4;¹⁰ with roughly similar exchange current densities considered for H_2CO_3 and H^+ ,¹² the expected contribution of H_2CO_3 falls easily within the experimental error of the measurements reported by the authors. In addition, while the use of additional buffer was an elegant way to elucidate the charge transfer cathodic currents, concerns could be raised about the secondary effects of these buffers on the electrochemical reactions.

In 2008, Remita, et al., studied the electrochemical activity of H_2CO_3 using a more quantitative approach.¹⁷ The authors conducted a series of experiments in N_2 -saturated and CO_2 -saturated solutions at pH ~ 4 using a rotating disk electrode (RDE) experimental apparatus. Their arguments were based on a comprehensive mathematical model, similar to those discussed above.¹³⁻¹⁵ Using the electrochemical kinetic parameters obtained for H^+ reduction in N_2 -saturated solutions, authors were able to predict the results obtained in CO_2 -saturated solutions without considering H_2CO_3 as a significant species (absent in their model). Their observation led to the conclusion that H_2CO_3 is not electrochemically active, and its sole effect was claimed to be the buffering effect of H_2CO_3 on surface concentration of H^+ . It is worthwhile to mention that the arguments used in this study suffer from the same shortcomings as those in the study by Linter and Burstein.¹⁶ That is the very narrow range of experimental conditions and the fact that at their conditions (pH 4 and 1 bar CO_2) the cathodic currents are dominated by H^+ reduction. In fact, one may suggest that the charge transfer controlled currents were not clearly observed as compared to the study of Linter and Burstein,¹⁶ where an additional buffer was used to shift the mass transfer limiting current toward higher values. At the conditions in the study by Remita, et al.,¹⁷ the observed range of cathodic currents were mostly under mixed charge transfer/mass transfer control, and the pure charge transfer controlled currents were covered by the anodic reaction at lower currents and by the mass transfer limiting current at higher currents. That makes the distinction of the

possible effect of electrochemical activity of H_2CO_3 even harder. The conclusion made by Remita, et al., that H_2CO_3 acts as a buffer in this system, is in agreement with what was suggested earlier—that the limiting current densities could be reasonably predicted without the direct reduction of H_2CO_3 .¹³⁻¹⁵ The effect of flow velocity that was discussed extensively, and the good agreement obtained with the model prediction is merely a further confirmation of the buffering ability of H_2CO_3 as a weak acid.

It is important to realize that the clearly demonstrated buffering ability of H_2CO_3 (or any other weak acid) does not exclude the possibility of H_2CO_3 direct reduction, as these are two independent processes. That is the reason why in order to distinguish them, the arguments must be based on the behavior of pure charge transfer controlled currents so that the electrochemical activity of H_2CO_3 can be separated from the chemical equilibria (buffering) associated with this species. This concept was not properly accounted for in the analysis of the surface pH measurements made by Remita, et al.¹⁷ Their results clearly showed that in the presence of H_2CO_3 the surface pH is lower than in a N_2 -saturated solution of the same pH. While this observation further confirms the buffering ability of H_2CO_3 , it provides no insight into the electrochemical activity of this species, as they claimed. In fact, considering the fast kinetics of $\text{H}^+/\text{HCO}_3^-$ recombination as compared to the CO_2 hydration,⁹⁻¹⁰ the surface pH is expected to be nearly identical irrespective of whether H_2CO_3 is reduced (to H_2 and HCO_3^-) or not. In brief, the study by Remita, et al., is of significance as it further elucidated the possible mechanisms underlying CO_2 corrosion by explicitly focusing on the buffering ability of H_2CO_3 . Nevertheless, the arguments and the experimental results did not provide sufficient evidence as it relates to electrochemical activity of H_2CO_3 .

In attempt to address the shortcomings of the previous studies, Tran, et al., conducted a series of experiments at elevated pressures up to 10 bar (1,000 kPa) CO_2 .¹⁸ At such conditions, the authors were able to investigate the electrochemical activity of H_2CO_3 , as the dominant chemical species, with more confidence. Nevertheless, it was noted that even at such high CO_2 partial pressures the charge transfer controlled currents could not be observed on X65 mild steel because of the interference of the anodic reaction at low current densities and the mass transfer limitation at the higher end. Therefore, the experiments were conducted on a Type 304 stainless steel (UNS S30400⁽¹⁾) surface. The suppressed anodic current densities on stainless steel surface allowed the cathodic charge transfer controlled currents to be observed clearly. The experimental results showed that the presence of H_2CO_3 , even at high levels (when

partial pressure of CO_2 [pCO_2] = 10 bar), did not result in any significant change of charge transfer controlled currents as measured on a stainless steel surface. This observation demonstrated that H_2CO_3 is not electrochemically active, at least not on the surface of stainless steel. While the experimental conditions of this study allowed a proper measurement and discussion of the electrochemical activity of H_2CO_3 , one must consider the fact that the two surfaces (actively corroding mild steel vs. the passive stainless steel) are very different. The presence of a significant amount of alloying elements (i.e., ~20% Cr, 10% Ni) raises the uncertainty about whether the electrochemical mechanisms identified on stainless steel can be simply assumed to be valid for mild steel surfaces. The mechanism and the kinetics of the hydrogen evolution reaction are known to be significantly influenced by the composition of the substrate and even by the fine differences in surface preparation procedures.¹⁹⁻²¹ Additionally, the passive oxide layer formed on stainless steel may alter the kinetics and the mechanism of the hydrogen evolution reaction,²² considering that the hydrogen evolution reaction (from H^+ or H_2CO_3) involves a series of surface dependent chemical/electrochemical adsorption/desorption steps.²³⁻²⁴

The review of the existing literature clearly shows that despite many decades of research on the mechanism of CO_2 corrosion, some important mechanistic aspects have remained unresolved. Among them is the electrochemical activity of H_2CO_3 . However, neither of the two competing ideas about the electrochemical activity of H_2CO_3 appears to have sufficient experimental evidence in their support so far. As identified previously,^{18,25-28} the direct experimental evidence for electrochemical activity of a weak acid (such as H_2CO_3) may be obtained by investigating the behavior of pure charge transfer controlled cathodic currents. If the reduction of H_2CO_3 is significant, at a fixed pH, the charge transfer controlled currents would increase as pCO_2 increases—as a result of increased H_2CO_3 concentration, and thus, increased rate of H_2CO_3 reduction reaction. On the other hand, if the charge transfer controlled currents remained unaffected by pCO_2 , it can be deduced that H^+ reduction is the dominant cathodic reaction and H_2CO_3 is not significantly electroactive.

It is apparent from the previous attempts on investigating the electrochemical activity of H_2CO_3 ¹⁶⁻¹⁸ that the main challenge in verifying these hypothetical behaviors is to create the experimental conditions required to observe the charge transfer controlled cathodic currents. In the present study, in addition to the experiments conducted in a conventional three-electrode glass cell test apparatus, a thin channel flow geometry, enabling high-flow velocities, was used in order to further increase the limiting currents. This was accentuated by lowering the temperature in order to disproportionately decrease the rates of electrochemical

⁽¹⁾ UNS numbers are listed in *Metals and Alloys in the Unified Numbering System*, published by the Society of Automotive Engineers (SAE International) and cosponsored by ASTM International.

TABLE 1
Chemical Composition of Steel Working Electrodes (wt%)

	S	Cu	P	V	C	Cr	Mo	Si	Ni	Mn	Co	Fe
API X65	0.009	—	0.009	0.047	0.13	0.25	0.16	0.26	0.29	1.16	—	Balance
Type 316L ^(A)	0.025	0.590	0.035	0.050	0.018	16.650	2.040	0.540	10.120	1.510	0.330	Balance

^(A) Other elements with less than 0.1 wt% concentrations: titanium, tin, tantalum, columbium, aluminum, boron, and vanadium.

reactions, making them the rate determining step, and also by increasing the pCO₂ above atmospheric pressures.

Measurements in the present study were conducted on three different surfaces: Type 316L stainless steel (UNS S31603), 99.9 wt% pure iron, and API 5L X65 mild steel. Mild steel is a typical material of choice for the transmission pipelines in the oil and gas industry, which is at focus in the present study. The stainless steel electrode was selected because of the same considerations as suggested by Tran, et al.,¹⁸ and also to provide an opportunity for the comparison with the previous studies.^{16,18} The choice of pure iron was made because of its close relevance with mild steel (which consists of ~98 wt% iron), when compared to stainless steel (~70 wt% iron), in order to provide further insight into the possible effect of alloying elements.

MATERIAL AND METHODS

The Glass Cell

A series of experiments were conducted in a 1 L glass cell, using a RDE, three-electrode test apparatus. The experimental setup is similar to that described for an earlier study.²⁶ The 0.1 M NaCl supporting electrolyte was purged with N₂ or CO₂ gas, depending on the type of experiment. The outlet gas was monitored with an oxygen sensor (Orbisphere 410[†]) to assure sufficient deoxygenation (~1 ppb_m dissolved oxygen). The solution pH was then adjusted to 4.0 using a small amount of diluted NaOH or HCl solutions. That was followed by further purging of the solution to maintain the minimal amount of dissolved oxygen content. The solution pH was monitored throughout all experiments to ascertain a constant value.

The RDEs with a 5 mm diameter were made of either 99.99 wt% pure iron or API X65 5L mild steel (composition in Table 1), press fitted into a Teflon^{TM†} electrode holder (Pine instruments). The electrodes were polished and electrochemically treated according to the procedure discussed elsewhere.²⁵

The cathodic polarization measurements were initiated from open-circuit potential (OCP) toward the more negative values after a stable OCP was observed (< ±2 mV drift over 5 min). The steady-state voltammograms were obtained using staircase voltammetry at 0.5 mV/s scan rate and 1 s⁻¹ sampling period. The

reported results are corrected for ohmic drop using the solution resistance obtained from electrochemical impedance spectroscopy (EIS) measurements performed after the polarization experiments (DC potential at OCP, AC potential ±5 mV, frequency range 10 kHz to 0.2 Hz at 8 points/decade). The linear polarization resistant (LPR) measurements were conducted in separate tests following the abovementioned preparation procedure. The measurements were done by sweeping the potential from 5 mV_{OCP} to -5 mV_{OCP}, using 0.125 mV/s scan rate and 1 s⁻¹ sampling period.

The Thin Channel Flow Cell

The detailed description of the thin channel flow cell (TCFC) used in the present study can be found in earlier publications.²⁹⁻³³ In the present study, the test section was slightly modified by introducing a saturated Ag/AgCl reference electrode, flush mounted on the lid, directly opposite to the working electrode, as shown in Figure 1. The cell structure was used as the counter electrode.

The 0.1 M NaCl solution (110 L) was made with deionized water and analytical grade chemicals. The solution was then purged for ~3 h, with N₂ or CO₂ gas, depending on the desired experimental conditions, while the outlet gas was monitored with an oxygen sensor to ensure proper deoxygenation. Maximum dissolved oxygen content, measured before initiating the experiment, was 3 ppb (typically ~1 ppb). In the high-pressure experiments, after the deoxygenation step, the system was pressurized to 5 bar (500 kPa) CO₂ and then maintained at that pressure until the solution became saturated, after at least 3 h. As the last step, the pH (measured by an OMEGA 5431-10[†] pH probe) was adjusted to the targeted value by gradual

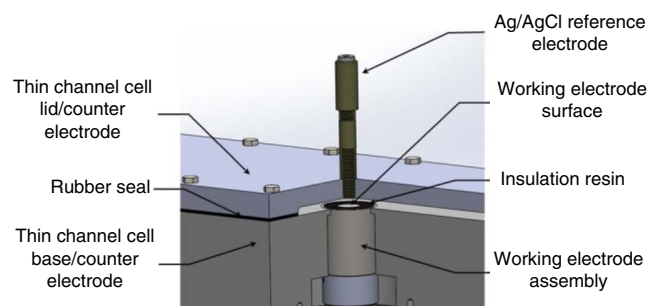


FIGURE 1. The illustration of the three-electrode cell arrangement inside the thin channel test section.

[†] Trade name.

addition of deoxygenated HCl or NaOH solution into the system from a secondary pressurized reservoir.

The experiments were conducted on three different substrates: 99.99 wt% pure iron, Type 316L stainless steel, and API 5L X65 mild steel. The chemical composition of the stainless steel and the mild steel are shown in Table 1. The working electrode assembly was built similarly to that shown in an earlier study,³³ with a single disk working electrode, which was mounted into the test section as shown in Figure 1.

Prior to each experiment, the working electrode was abraded with a 600 grit silicon carbide paper, then rinsed and sonicated for 5 min using isopropanol. The working electrode was flush-mounted on the bottom of the thin channel test section, which was then closed and purged with dry CO₂ or N₂. In the case of mild steel and pure iron electrodes, after exposing the electrode to the test solution, the OCP was monitored until a steady value was reached prior to initiating polarization measurements. For the experiments on the stainless steel surface, the polarization measurements were initiated 2 min after exposing the electrode to the test solution in order to avoid any significant passivation of the electrode. The polarization curves were obtained using the same electrochemical measurement parameters as those in the glass cell experiments.

The solution temperature was controlled within $\pm 0.5^\circ\text{C}$ by using a jacketed immersion heater located in the tank and covered cartridge heaters used to directly heat the test section (for experiments conducted at 30°C), as well as a shell and tube heat exchanger connected to a chiller (Air 3000[†] FLUID CHILLERS, Inc.) for experiments done at 10°C. The flow velocity inside the thin channel test section was fixed at 13 m/s throughout the experiments.

All experiments in this study were repeated at least three times. The results shown in the following are the average values of all repeats at certain potential intervals. The error bars represent the minimum and maximum measured values.

RESULTS AND DISCUSSION

The steady-state cathodic polarization curves obtained in glass cell experiments are presented in Figures 2 and 3. These experiments were conducted in order to examine whether the conditions typical for glass cell experiments allow a proper discussion of the electrochemical activity of H₂CO₃. All of the polarization curves reported in the present study (obtained in both glass cell and TCFC) demonstrate the same generic trend. A steep increase in current is seen just below the OCP, followed by the limiting current and a linearly increasing current density range at even lower potentials that are associated with the water reduction reaction.

Figure 2 shows the comparison of the cathodic polarization curves obtained in a N₂-saturated solution

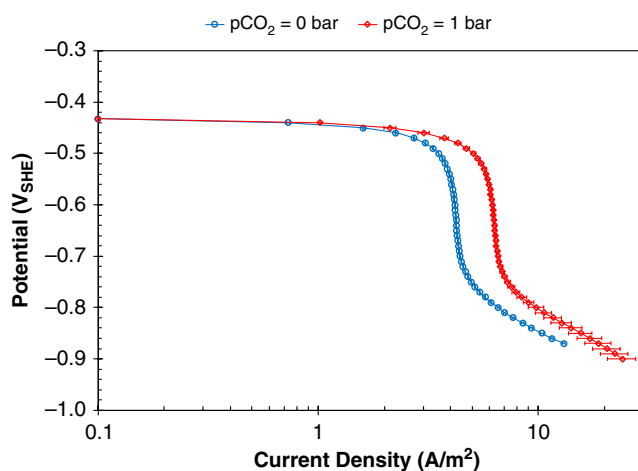


FIGURE 2. Steady-state cathodic polarization curves obtained at 30°C, pH 4.0, 2,000 rpm RDE on API 5L X65 mild steel, in N₂-saturated and CO₂-saturated solutions.

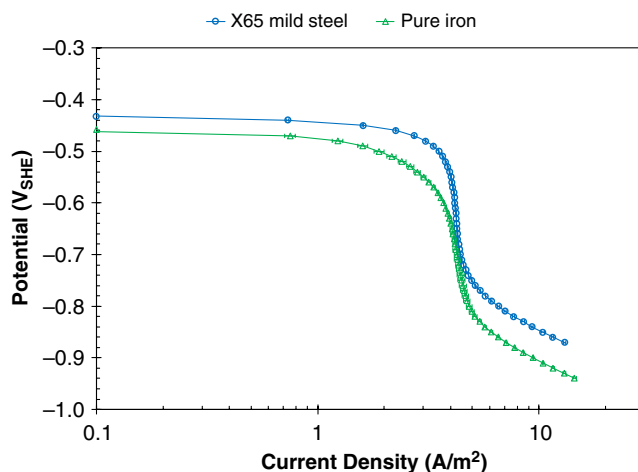


FIGURE 3. Steady-state cathodic polarization curve obtained at 30°C, pH 4.0, 2,000 rpm RDE in N₂-saturated solution on API 5L X65 mild steel and 99.99 wt% pure iron electrodes.

at pH 4.0 with a CO₂-saturated solution at the same pH. The results show a clear increase of the limiting current in CO₂-saturated solutions. As discussed above, this increase is stemming from the presence of carbonic acid, and the CO₂ hydration reaction, which can be readily explained irrespective of whether H₂CO₃ is electrochemically active or not. The focus in the present study is on the charge transfer controlled cathodic currents, where the surface concentrations of species are the same as the bulk solution. At such conditions, homogeneous chemical dissociation of H₂CO₃ has no influence on the current/potential response of the system. Therefore, the surface concentration of H₂CO₃ depends only on pCO₂ and temperature. Consider the dissolution and hydration equilibria:⁹

$$[\text{H}_2\text{CO}_3] = K_{\text{hyd}}K_{\text{dis}}p\text{CO}_2 \quad (10)$$

where the brackets denote equilibrium concentration in M, and $K_{\text{hyd}} = 1.18 \times 10^{-3}$ and $K_{\text{dis}} = 2.96 \times 10^{-2}$ M/bar are the equilibrium constants of the hydration reaction (Reaction [2]) and dissolution reaction (Reaction [1]) at 30°C, respectively.³⁴⁻³⁵ Thus, for $p\text{CO}_2 = 0.96$ bar (96 kPa), the $[\text{H}_2\text{CO}_3] = 3.35 \times 10^{-5}$ M. At these conditions, H^+ is the dominant electroactive species with a three-fold higher concentration than H_2CO_3 . Hence, the theoretical difference expected from the two proposed mechanisms—one with and the other without the direct reduction of H_2CO_3 —is very small when compared to the typical experimental error.

Furthermore, the polarization curves shown in Figure 2 do not demonstrate a distinguishable charge transfer controlled current range, in either of the solutions. In fact, the LPR measurement in CO_2 -saturated solution estimated the corrosion current to be 1.81 A/m^2 (based on Stern-Geary equation with B value = 13 mV). The comparison of this value with the mass transfer limiting current of 6.34 A/m^2 suggests that even in CO_2 -saturated solution the observed cathodic polarization curve is significantly under the influence of the limiting current. Remembering that the limiting current density is identical for both mechanisms, a simple comparison can be made based on:

$$\frac{1}{i} = \frac{1}{i_{\text{ct}}} + \frac{1}{i_{\text{lim}}} \quad (11)$$

which suggests that in a mixed charge transfer/mass transfer regime, the theoretical difference between the two aforementioned mechanisms is even smaller. Therefore, the results obtained in typical glass cell experiments, which are similar to those reported previously,¹⁶⁻¹⁷ do not allow for a proper mechanistic discussion on the electrochemical activity of H_2CO_3 . In order to examine the electrochemical activity of H_2CO_3 , the experiments were continued in the TCFC test apparatus, where more suitable experimental conditions could be achieved, as described further below.

The influence of substrate composition on the electrochemical response of the system was also examined briefly in the glass cell experiments. The cathodic polarization curve obtained on 99.99 wt% pure iron in N_2 -saturated solution is compared with that obtained on API 5L X65 mild steel surface in Figure 3. While the reproducibility of the results obtained on a pure iron surface was slightly lower when compared to steel, the polarization curves showed that the pure iron surface is a significantly weaker catalyst for the reduction reactions, in agreement with previous reports.^{25,36} Considering that the pure charge transfer controlled currents for H^+ reduction were not observed, the true difference in the electrocatalytic effect of the two surfaces cannot be properly distinguished

here. Nevertheless, the observed difference even in this mixed mass transfer/charge transfer controlled regime signifies the importance of the substrate composition when discussing the electrochemical kinetics and mechanisms.

The following experiments that were conducted in the TCFC test apparatus had two main advantages: the ability to increase the flow velocity to significantly higher values in order to increase the mass transfer limitation and the ability to conduct the experiments at elevated $p\text{CO}_2$ (5 bar maximum operating pressure), hence, increasing the concentration of H_2CO_3 . Figure 4 shows the cathodic polarization curves obtained at 30°C in the TCFC.

The cathodic polarization curves obtained on Type 316L stainless steel electrodes are shown in Figure 4(a). The results clearly demonstrate the charge transfer controlled currents, in a wide potential range. This range of current densities was not affected by increasing the $p\text{CO}_2$ from 0 bar to 5 bar, suggesting that H_2CO_3 reduction on stainless steel is not significant at these conditions. The sole effect of H_2CO_3 was buffering the H^+ concentration, and hence, increasing of the limiting current. These experimental results were found to be in agreement with those reported previously.^{16,18} The limiting currents in Figure 4(a) show an increase in presence of CO_2 . However, the increase of $p\text{CO}_2$ from 0 bar to 1 bar resulted only in a slight increase in limiting current densities. That is a result of the overwhelmingly high mass transfer flux of H^+ . As $p\text{CO}_2$ increased further to 5 bar, the concentration of H_2CO_3 increased and the effect of CO_2 hydration reaction became more pronounced, leading to a significantly higher limiting current density.

The cathodic polarization behavior on pure iron electrodes is shown in Figure 4(b). The charge transfer controlled currents were also clearly observed over a reasonably extended potential range. On the iron surface, the reproducibility of the results decreased, which is indicated by the larger error bars. The charge transfer controlled cathodic currents appear to show a slight variation at different $p\text{CO}_2$; however, this is not conclusive because of the magnitude of the error bars. The comparison of the polarization curves, especially those obtained at 5 bar $p\text{CO}_2$ (where carbonic acid is the dominant species) with those at 0 bar CO_2 , does not indicate any significant electrochemical activity for H_2CO_3 .

The cathodic polarization curves obtained on an API 5L X65 mild steel surface are shown in Figure 4(c). The comparison of the mass transfer limiting currents obtained in N_2 -saturated solutions with those obtained in glass cell experiments at similar conditions (Figure 2) show more than a five-fold increase in mass transfer limiting current (22.9 A/m^2 vs. 4.2 A/m^2), yet the charge transfer controlled current range was still not observed clearly. With increase of $p\text{CO}_2$ to 1 bar, the charge transfer controlled range

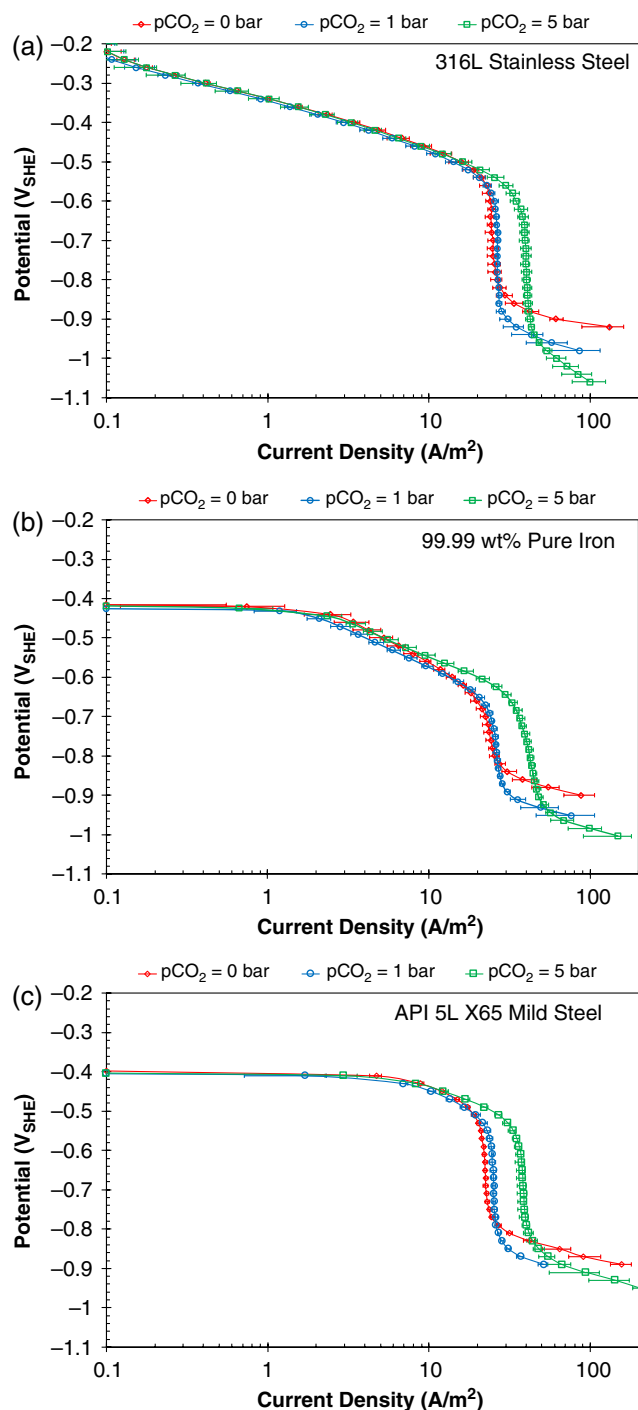


FIGURE 4. Steady-state cathodic polarization curves at pH 4, 30°C, 13 m/s TCFC, 0.1 M NaCl, 0.5 mV/s scan rate. (a) Type 316L stainless steel, (b) 99.99 wt% pure iron, and (c) API 5L X65 mild steel.

gradually appeared and it is seen clearly at $p\text{CO}_2 = 5$ bar. On the mild steel surface, the pure charge transfer controlled currents were observed in a rather narrow range of potentials, as compared to those on stainless steel and iron surfaces. Nevertheless, the comparison of the results at 1 bar and 5 bar CO_2 does not indicate significantly higher current densities in

that range, favoring the arguments that H_2CO_3 is not electrochemically active on API 5L X65 mild steel either.

In order to extend the range of charge transfer controlled currents on the API 5L X65 mild steel surface and solidify the mechanistic arguments above, similar experiments were conducted at 10°C. Decreasing the temperature was expected to reduce the rates of electrochemical reactions more than the limiting currents. Such a disproportional decrease would allow the charge transfer controlled currents to be observed in a wider range. That is shown to be the case in Figure 5, where the cathodic polarization curves obtained in N_2 -saturated solutions at 10°C and 30°C are compared. At 10°C, the rate of H^+ reduction reaction is decreased almost by an order of magnitude.

The effect of $p\text{CO}_2$ on the charge transfer controlled current densities obtained on API 5L X65 mild steel at 10°C is shown in Figure 6. At this condition the charge transfer controlled currents on mild steel were clearly observed and showed no significant dependence on $p\text{CO}_2$. The results obtained at 10°C were, therefore, found to further support the previous observation that the direct reduction of H_2CO_3 on a mild steel surface is insignificant.

The polarization curves obtained on the three different surfaces are compared in Figure 7 for solutions at 5 bar CO_2 and 30°C, where the pure charge transfer controlled currents were observed on all three substrates. The results show a significant effect of the surface composition on the observed electrocatalytic activity related to H^+ reduction, in the following order: mild steel > stainless steel > pure iron. Such a large difference in the electrocatalytic behavior of different substrates may result in different electrochemical mechanisms, especially considering that the investigated reactions are multi-step and include different adsorption/desorption elementary reactions. In that

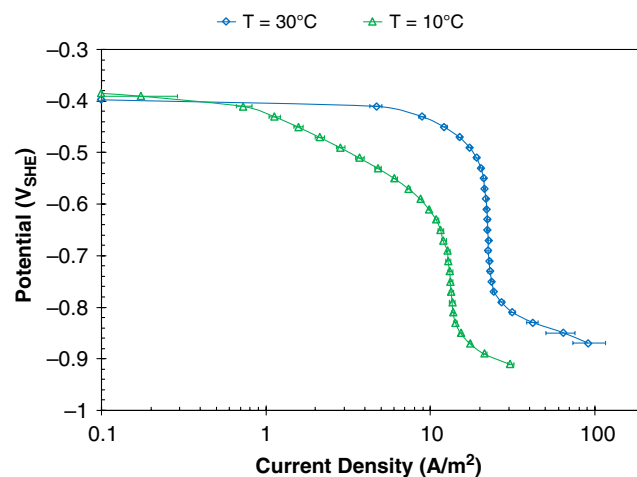


FIGURE 5. The effect of temperature on steady-state cathodic polarization curve obtained on API 5L X65 mild steel in N_2 -saturated solution at pH 4.0, 13 m/s TCFC, 0.1 M NaCl, 0.5 mV/s.

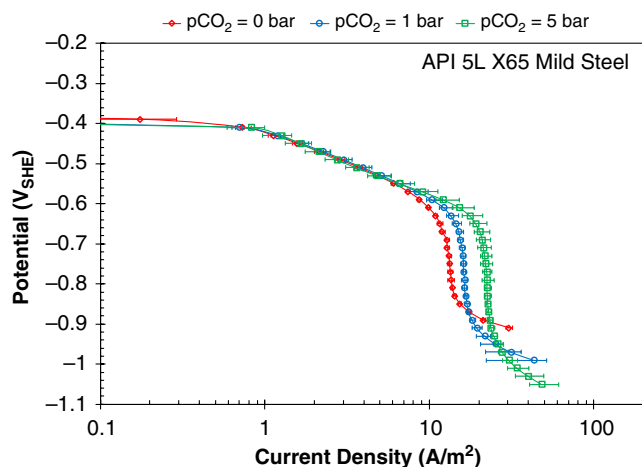


FIGURE 6. Steady-state cathodic polarization curves at pH 4.0, 10°C, 13 m/s TCFC, 0.1 M NaCl, 0.5 mV/s scan rate on an API 5L X65 mild steel surface.

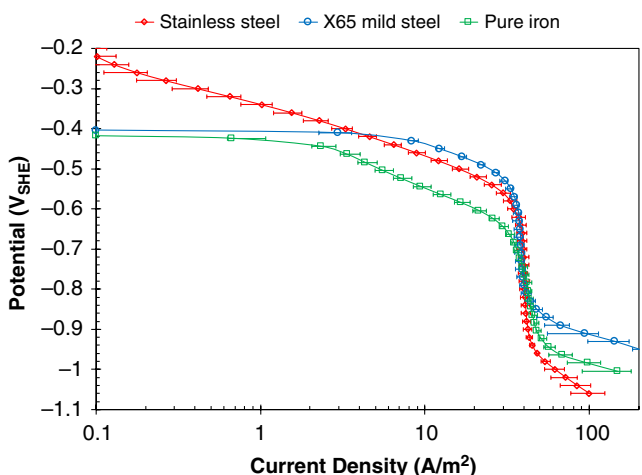


FIGURE 7. The comparison of the steady-state cathodic polarization curves obtained on API 5L X65 mild steel, Type 316L stainless steel, and 99.99 wt% pure iron at pH 4, 30°C, 13 m/s TCFC, 0.1 M NaCl, 0.5 mV/s scan rate.

case, even a small change in the adsorption energies of the intermediate species may result in different mechanistic behavior. Hence, while the choice of different substrates may be an appealing approach to investigate the electrochemical mechanisms, the complication introduced by different electrocatalytic properties requires a careful verification of the results on the substrate of interest.

In the present study, the cathodic polarization behavior of CO₂-saturated solutions at pH 4.0 and pCO₂ up to 5 bar was investigated on pure iron, stainless steel, and mild steel surfaces. The experimental results obtained on all three substrates suggest that H₂CO₃ reduction was not significant at the conditions considered here, in support of the recent mechanistic arguments found in the literature.¹⁶⁻¹⁸ Therefore, the

cause of higher corrosion rates in CO₂-saturated brines has to be sought elsewhere. In a recent study,³⁷ focused on the iron dissolution reaction, the presence of CO₂ was found to significantly increase the observed anodic currents. From these observations, it appears that the underlying mechanism of CO₂ corrosion is yet to be fully established.

CONCLUSIONS

❖ The cathodic polarization behavior of acidic CO₂-saturated solutions at pH 4.0 was investigated on 99.99 wt% pure iron, Type 316L stainless steel, and API 5L X65 mild steel surfaces, using a conventional three-electrode glass cell and a thin channel flow cell. The charge transfer controlled currents were observed most clearly at high flow rates and lower temperatures achieved in the thin channel flow cell. The cathodic currents obtained on all three substrates showed no indication of direct reduction of carbonic acid up to pCO₂ = 5 bar. The comparison of the polarization behavior on the three substrates showed a significant difference in their electrocatalytic activity when it comes to H⁺ reduction, with the API 5L X65 mild steel being most active, followed by Type 316L stainless steel, and with 99.99 wt% pure iron being least active.

ACKNOWLEDGMENTS

The authors would like to thank the following companies for their financial support: Anadarko, Baker Hughes, BP, Chevron, CNOOC, ConocoPhillips, DNV GL, ExxonMobil, M-I SWACO (Schlumberger), Multi-Chem (Halliburton), Occidental Oil Company, Petrobras, PTT, Saudi Aramco, Shell Global Solutions, SINOPEC (China Petroleum), TransCanada, TOTAL, and Wood Group Kenny.

REFERENCES

1. S. Nešić, "Carbon Dioxide Corrosion of Mild Steel," in *Uhlig's Corrosion Handbook*, 3rd ed. (Hoboken, NJ: John Wiley & Sons, 2011), p. 229-245.
2. S. Nešić, *Corros. Sci.* 49 (2007): p. 4308-4338.
3. M.B. Kermani, A. Morshed, *Corrosion* 59 (2003): p. 659-683.
4. C. de Waard, D.E. Milliams, "Prediction of Carbonic Acid Corrosion in Natural Gas Pipelines," International Conference Proceedings: Internal and External Protection of Pipes (Cranfield, England: BHRA, 1975), p. F1-1-F1-8.
5. C. de Waard, D.E. Milliams, *Corrosion* 31 (1975): p. 177-181.
6. G. Schmitt, B. Rothmann, *Werkst. Korros.* 28 (1977): p. 816.
7. L.G.S. Gray, B.G. Anderson, M.J. Danysh, P.R. Tremaine, "Mechanisms of Carbon Steel Corrosion in Brines Containing Dissolved Carbon Dioxide at pH 4," CORROSION 1989, paper no. 464 (Houston, TX: NACE International, 1989).
8. L.G.S. Gray, B.G. Anderson, M.J. Danysh, P.R. Tremaine, "Effect of pH and Temperature on the Mechanism of Carbon Steel Corrosion by Aqueous Carbon Dioxide," CORROSION 1990, paper no. 40 (Houston, TX: NACE, 1990).
9. A. Kahyarian, M. Singer, S. Nestic, *J. Nat. Gas Sci. Eng.* 29 (2016): p. 530-549.
10. A. Kahyarian, M. Achour, S. Nestic, "Mathematical Modeling of Uniform CO₂ Corrosion," in *Trends in Oil and Gas Corrosion*

- Research and Technologies*, ed. A.M. El-Sherik (Amsterdam, Netherlands: Elsevier, 2017), p. 805-849.
11. A. Kahyarian, M. Achour, S. Nestic, "CO₂ Corrosion of Mild Steel," in *Trends in Oil and Gas Corrosion Research and Technologies*, ed. A.M. El-Sherik (Amsterdam, Netherlands: Elsevier, 2017), p. 149-190.
 12. S. Nešić, J. Postlethwaite, S. Olsen, *Corrosion* 52 (1996): p. 280-294.
 13. M. Nordsveen, S. Nešić, R. Nyborg, A. Stangeland, *Corrosion* 59 (2003): p. 443-456.
 14. B.F.M. Pots, "Mechanistic Models for the Prediction of CO₂ Corrosion Rates Under Multi-Phase Flow Conditions," CORROSION 1995, paper no. 137 (Houston, TX: NACE, 1995).
 15. S. Turgoose, R.A. Cottis, K. Lawson, "Modeling of Electrode Processes and Surface Chemistry in Carbon Dioxide Containing Solutions," in *Computer Modeling in Corrosion*, ASTM STP 1154 (West Conshohocken, PA: ASTM International, 1992), p. 67-81.
 16. B.R. Linter, G.T. Burstein, *Corros. Sci.* 41 (1999): p. 117-139.
 17. E. Remita, B. Tribollet, E. Sutter, V. Vivier, F. Ropital, J. Kittel, *Corros. Sci.* 50 (2008): p. 1433-1440.
 18. T. Tran, B. Brown, S. Nešić, "Corrosion of Mild Steel in an Aqueous CO₂ Environment—Basic Electrochemical Mechanisms Revisited," CORROSION 2015, paper no. 671 (Houston, TX: NACE, 2015).
 19. E. Bus, J.A. van Bokhoven, *Phys. Chem. Chem. Phys.* 9 (2007): p. 2894-2902.
 20. J.O. Bockris, D.F.A. Koch, *J. Phys. Chem.* 65 (1961): p. 1941-1948.
 21. S.Y. Qian, B.E. Conway, G. Jerkiewicz, *J. Chem. Soc. Faraday Trans. 94* (1998): p. 2945-2954.
 22. N.T. Thomas, K. Nobe, *J. Electrochem. Soc.* 117 (1970): p. 622.
 23. A. Kahyarian, B. Brown, S. Nestic, *J. Electrochem. Soc.* 164 (2017): p. 365-374.
 24. B.E. Conway, B.V. Tilak, *Electrochim. Acta* 47 (2002): p. 3571-3594.
 25. A. Kahyarian, B. Brown, S. Nestic, *Corrosion* 72 (2016): p. 1539-1546.
 26. A. Kahyarian, A. Schumaker, B. Brown, S. Nestic, *Electrochim. Acta* 258 (2017): p. 639-652.
 27. T. Tran, B. Brown, S. Nestic, B. Tribollet, *Corrosion* 70 (2014): p. 223-229.
 28. T. Hurlen, S. Gunvaldsen, F. Blaker, *Electrochim. Acta* 29 (1984): p. 1163-1164.
 29. F. Farelas, M. Galicia, B. Brown, S. Nestic, H. Castaneda, *Corros. Sci.* 52 (2010): p. 509-517.
 30. Y. Yang, "Removal Mechanisms of Protective Iron Carbonate Layer in Flowing Solutions" (Ph.D. dissertation, Ohio University, 2012).
 31. W. Li, "Mechanical Effects of Flow on CO₂ Corrosion Inhibition of Carbon Steel Pipelines" (Ph.D. dissertation, Ohio University, 2016).
 32. W. Li, B.F.M. Pots, B. Brown, K.E. Kee, S. Nestic, *Corros. Sci.* 110 (2016): p. 35-45.
 33. F. Farelas, B. Brown, S. Nestic, "Iron Carbide and Its Influence on the Formation of Protective Iron Carbonate in CO₂ Corrosion of Mild Steel," CORROSION 2013, paper no. 2291 (Houston, TX: NACE, 2013).
 34. A.L. Soli, R.H. Byrne, *Mar. Chem.* 78 (2002): p. 65-73.
 35. D. Li, Z. Duan, *Chem. Geol.* 244 (2007): p. 730-751.
 36. J.O. Bockris, D. Drazic, *Electrochim. Acta* 7 (1962): p. 293-313.
 37. A. Kahyarian, B. Brown, S. Nestic, *Corros. Sci.* 129 (2017): p. 146-151.